IBRO Neuroscience Reports 17 (2024) 177–187

Contents lists available at ScienceDirect

IBRO Neuroscience Reports

journal homepage: www.sciencedirect.com/journal/IBRO-Neuroscience-Reports

IL-33 relieves nerve injury by mediating microglial polarization in neuromyelitis optica spectrum disorders via the IL-33/ST2 pathway

Lu Huang [a,b], Congcong Fu [a,b], Sha Liao [a,b], Youming Long [a,b,*]

[a] Department of Neurology, the Second Affiliated Hospital of Guangzhou Medical University, 250# Changgang East Road, Guangzhou, Guangdong 510260, China
[b] Department of Neurology, Institute of Neuroscience, Key Laboratory of Neurogenetics and Channelopathies of Guangdong Province and the Ministry of Education of China, the Second Affiliated Hospital of Guangzhou Medical University, Guangzhou, Guangdong 510260, China

ARTICLE INFO

Keywords:
NMOSD
Microglia
IL-33
AQP4
ST2

ABSTRACT

Interleukin-33 (IL-33) is a member of the interleukin-1 cytokine family. Its function in regulating microglial M1/M2 polarization in neuromyelitis optica spectrum disorder (NMOSD) is still unelucidated. To evaluate the role of IL-33 in NMOSD, we constructed NMOSD mice model by injecting purified serum IgG from AQP4-IgG seropositive NMOSD patients into experimental autoimmune encephalomyelitis (EAE) mice, and IL-33 was intraperitoneally injected into NMOSD mice 3 d before the model induction. We found that pretreatment of the NMOSD mice with IL-33 relieved brain neuron loss, and demyelination and improved the structure of axons, astrocytes, and mitochondria. In the neuronal and microglial coculture system, pretreatment with IL-33 in microglia alleviated NMOSD serum-induced inflammation and damaged morphology in cultured neurons. IL-33 transformed microglia to the M2 phenotype, and NMOSD serum promoted microglia to the M1 phenotype in cultured BV2 cells. Moreover, IL-33 influenced microglial polarity via the IL-33/ST2 pathway. IL-33 may be a novel insight useful for further developing NMOSD-targeted therapy and drug development.

Introduction

NMOSD, a severe inflammatory autoimmune CNS disorder triggered by the binding of AQP4-IgG to the aquaporin four water channel on the end-feet of astrocytes, primarily attacks the spinal cord and optic nerves (Misu et al., 2007). In addition to AQP4 loss, neuronal injury, and demyelination, microglial activation is prominent in the AQP4-rich CNS regions, as observed in the histopathology of NMOSD lesions (Guo et al., 2017; Lucchinetti et al., 2014; Chen et al., 2021). Agnieszka et al. discovered that type I interferon-activated microglia play a crucial role in the pathology of NMOSD (Wlodarczyk et al., 2021). A recent study reported that astrocyte–microglial interaction, mediated by C3-C3aR signaling, is a driver of NMOSD pathogenesis in mice models, and microglia may be the potential targets for NMOSD (Chen et al., 2020). Although microglia are activated and play a key role in NMOSD pathology, the mechanism underlying microglial polarization in NMOSD remains unelucidated to date.

Interleukin (IL)-33, a member of the IL-1 cytokine family, is a key immune modulator associated with various immune-mediated disorders (Vainchtein et al., 2018). A previous study revealed that serum IL-33 levels in NMOSD patients were significantly higher than those in healthy controls, and serum IL-33 levels during the acute phase were associated with more past attacks in NMOSD patients (Zhang et al., 2018). Yao et al. found that serum albumin (SA) concentration was significantly correlated with EDSS score in NMOSD patients in the acute phase but not in the remission phase, and SA was negatively correlated with the serum level of IL-33 in the acute phase of NMOSD (Yao et al., 2020). A recent study found that IL-33 may induce dysfunction of the blood brain barrier and lead to intrathecal synthesis of immunoglobulin in the AQP4+NMOSD and MOGAD (Wang et al., 2023). All the studies

Abbreviations: NMOSD, neuromyelitis optica spectrum disorder; ST2, stimulated expression gene 2; AQP4, aquaporin 4; IL-33, interleukin –33; HCs, healthy controls; MEM, minimum essential medium; SD, Sprague Dawley; EAE, experimental autoimmune encephalitis myelitis; MOG_{35-55}, myelin oligodendrocyte glycoprotein $_{35-55}$; TEM, transmission electron microscopy; PBS, phosphate-buffered saline; LFB, Luxol fast blue; PSD 95, postsynaptic density protein 95; TLR, toll-like receptor; IGF-1, insulin-like growth factors-1; BDNF, brain-derived neurotrophic factor; EGF, epidermal growth factor; Ilc2, innate lymphoid cells; SA, serum albumin; EDSS, expanded disability status scale; PTX, Pertussis toxin.

* Corresponding author at: Department of Neurology, the Second Affiliated Hospital of Guangzhou Medical University, 250# Changgang east Road, Guangzhou, Guangdong 510260, China.
E-mail address: youminglong@126.com (Y. Long).

https://doi.org/10.1016/j.ibneur.2024.07.008
Received 15 February 2024; Received in revised form 8 June 2024; Accepted 30 July 2024
Available online 3 August 2024

indicated a correlation between serum IL-33 concentration and the severity of NMOSD, but the underlying mechanism is unclear.

In the current study, pretreatment with IL-33 was found to ameliorate brain neuron loss, and demyelination and improve the structure of axons, astrocytes, and mitochondria in NMOSD mice. IL-33 pretreatment alleviated NMOSD serum-induced inflammation and neuron damage in the cocultured system. Meanwhile, IL-33 transformed microglia to M2 phenotype in cultured BV2 cells, which was dependent on ST2.

Materials and methods

Study participants

A total of seven healthy controls (HCs) and seven NMOSD patients who fulfilled the diagnostic criteria and with AQP4-IgG titers above 1:100 were enrolled in the study. Serum AQP4 auto-antibodies were detected using cell-based assays as described in previous reports (Long et al., 2017; Fu et al., 2022). All samples were collected before treatment and were frozen at –80 °C until use. Written informed consent was obtained from all participants. This study was approved by the committees for ethical review of research involving human subjects at the Second Affiliated Hospital of Guangzhou Medical University (Guangzhou, China).

Cell culture

Mouse microglia cells (BV2) were purchased from the China Center for Type Culture Collection in Shanghai, China. The cells were cultured in minimum essential medium (MEM) complete medium containing 10 % fetal bovine serum. ST2 knockdown BV2 cells were purchased from Cyagen Biosciences Inc, China. Sprague Dawley (SD) embryonic rats (16 d) were used to prepare neuronal cells. In brief, the pregnant rats were euthanized, and the fetal rats were isolated. Then, the brain tissue of the embryos was extracted and placed into precooled D-Hanks solution. After digestion with trypsin for 15 min and subsequent centrifugation, the extracted tissue was incubated with a 97 % neurobasal, 2 % 50× B-27, and 1 % penicillin—streptomycin solution in a 37 °C incubator with 5 % CO_2 (Pacifici and Peruzzi, 2012).

Pretreatment experiment

Recombinant murine IL-33 was purchased from Pepro Tech (catalog# 210–33) and was dissolved in PBS. To identify the optimal IL-33 concentration, the BV2 cells were seeded into 6-well cell culture plates at an initial density of 1×10^6 cells/mL. After culturing for 24 h, IL-33 was added to the cells at different concentrations (50, 100, and 200 ng/mL). After 24-h incubation, the cells were collected, total protein was extracted, and the Iba-1 expression levels were analyzed by Western blotting.

BV2 cells were seeded into 6-well cell culture plates and treated with MEM complete medium, IL-33 (100 ng/mL), and NMOSD serum (10 %). After incubation for 24 h, the effects of NMOSD serum and IL-33 on the BV2 cells were investigated.

Coculture assay

For the IL-33-NMOSD serum group, BV2 cells were seeded in a Transwell chamber and pretreated with IL-33 (100 ng/mL) or MEM media. After 24-h incubation, the BV2 cells were treated with NMOSD serum (10 %) and then cocultured with rat primary cortical neurons for 48 h.

ELISA

ELISA kits for IL-1β, IL-6, TNF-α, and IL-10 were purchased from RayBiotech, China, and the experiments were conducted following the manufacturers' instructions.

Clinical EAE scoring

Clinical EAE scores followed the standard EAE clinical disease scoring scale as described in a previous report (Hasselmann et al., 2017): 0 = No clinical signs; 0.5 = Some loss of tail tone; 1 = Complete tail limpness, with no evidence of limb weakness; 2.0 = No hind limb paralysis upon ambulation; 3.0 = Partial paralysis of hind limbs; 4.0 = Complete paralysis of both hind limbs; 5.0 = Immobile and unresponsive or death.

Establishment of the NMOSD model

Forty adult female C57/BL6 mice aged 6–8 weeks were purchased from Guangdong Medical Laboratory Animal Center. All mice were maintained on a standard 12-h light/dark cycle (8:00–20:00 light period) in a temperature-controlled room (21 ±25 °C) and were given free access to food and water. All animal experiments were conducted in accordance with the regulations of the Administration of Affairs Concerning Experimental Animals (China) and were approved by the Guangzhou Medical University Animal Ethics Committee.

The NMOSD model was established by the intraperitoneal injection of AQP4-IgG into the EAE mouse models (Saini et al., 2013). To establish the EAE model, thirty C57BL/6 female mice were immunized with a synthetic myelin oligodendrocyte glycoprotein 35–55 ($MOG_{35–55}$) polypeptide. After 10 days of $MOG_{35–55}$ injection, twenty of the thirty mice were intraperitoneally injected with 4 mg of human IgG each mouse purified from 3 AQP4-IgG positive NMOSD serum samples. Serum AQP4 antibodies of the 3 NMOSD patients were detected using cell-based assays as previously described (Long et al., 2017), and AQP4-IgG titers from 1:100 to over 1:1000. None of the 3 AQP4-IgG positive NMOSD patients were seropositive for anti-MOG antibodies. None of the 3 AQP4-IgG positive NMOSD patients had been treated with acetylsalicylic acid, thiazide diuretics, steroids, or other drugs that could affect protein levels within the previous 12 weeks, and none of the patients were diagnosed with diabetes mellitus, renal disorders, hepatic disorders, or malignancies. After 7 d of continuous injection, pathological changes in the NMOSD mouse models were studied.

Western blot

The total proteins of cells and tissues were extracted using protease inhibitor-containing RIPA buffer for 30 min on ice. The samples were centrifuged at 13,000 × g for 15 min at 4 °C. Then, the supernatants were collected, separated by SDS—PAGE, and transferred onto PVDF membranes. After blocking the membrane with TBST + 5 % BSA, the membrane was incubated with specific primary (Iba-1, 1:2000, Abcam, CD206, Abcam, 1:1000, CD40, Abcam, 1:1000 and β-actin, Boster, 1:3000) and secondary antibodies (1:5000, Abcam, USA). Finally, the target protein bands were visualized using an enhanced chemiluminescence assay (PerkinElmer, USA). The gray values were analyzed using image processing (Adobe, USA) and analysis programs (SPSS, USA).

Transmission electron microscopy

For fixation, the injured brain tissue was immersed in chilled 4 % glutaraldehyde and 1 % acetic acid. This was followed by washes with phosphate-buffered saline (PBS) and dehydration in an acetone gradient. The tissue was embedded in epoxy resin and sectioned. After negative staining with lead citrate, the sections were observed under a transmission electron microscope (HITACHI, Japan). We randomly selected 30 axons from each group, used professional image analysis software (Image-Pro Plus, IPP) to measure the diameter of the myelin

sheath and axon, and calculated the G-ratio [(axon diameter) /(axon diameter + myelin sheath diameter)] to evaluate demyelination (Sun et al., 2021).

Luxol Fast Blue

The brain sections were dehydrated and stained with Luxol Fast Blue (LFB). After washing, the demyelination of the cells was evaluated using a microscope.

RNA-Seq, data processing and quantitative real-time polymerase chain reaction

Total RNA was isolated using the Trizol Reagent (Invitrogen Life Technologies), after which the concentration, quality and integrity were determined using a NanoDrop spectrophotometer (Thermo Scientific). To select cDNA fragments of the preferred 400–500 bp in length, the library fragments were purified using the AMPure XP system (Beckman Coulter,Beverly, CA, USA). DNA fragments with ligated adaptor molecules on both ends were selectively enriched using Illumina PCR Primer Cocktail in a 15 cycle PCR reaction. Products were purified (AMPure XP system) and quantified using the Agilent high sensitivity DNA assay on a Bioanalyzer 2100 system (Agilent). The sequencing library was then sequenced on NovaSeq 6000 platform (Illumina) Shanghai Personal Biotechnology Cp. Ltd. Differential expression analyses were performed with R and Bioconductor packages of edgeR. The threshold required for the genes to be considered significantly changed was as follows: expression difference multiple $|\log2FoldChange| > 1$, significant P-value < 0.05.

For QPCR, cDNA was synthesized by reverse transcription using RNA as a template. The relative expression levels of the target genes were defined as $F = 2-\Delta\Delta ct$. The forward primers for ST2 were 5'-TGTATTTGACAGTTACGGAGGGC-3', the reverse primers for ST2 were 5'- ACTTCAGACGATCTCTTGAGACA-3'.

Immunofluorescence

The mouse brain sections were deparaffinized and rehydrated in xylene and ethanol. Endogenous peroxidase was quenched by incubation the sections in 3 % hydrogen peroxide, and antigen retrieval was performed in 0.01 M citrate buffer. The sections were then blocked and incubated with primary antibodies, namely, AQP4 (1:200 dilution, 16473–1-AP, PTG), Neun (1:200 dilution, CY5515, Abways), overnight at 4 °C. After the slices were rewarmed at RT for 60 min, they were incubated with Cy3-labeled donkey anti-rabbit IgG (1:500 dilution, 111–165–003, Jackson). Then, the slices were sealed with DAPI solution. Representative images were obtained with an automatic digital slide scanner (PANNORAMIC MIDI, 3DHISTECH), and Image J was used to determine the expression of the abovementioned proteins in the selected area for further data analysis.

For protein immunoreactivity in cells, the primary cortical neurons or BV2 cells were fixed with 4 % paraformaldehyde for 30 min at RT and treated with 0.5 % Triton for 10 min. After being washed with PBS, the cells were blocked with 5 % bovine

serum albumin (BSA) for 1 h and then incubated with a rabbit anti-PSD95 antibody (1:100 dilution, PA2295, Boster), anti-CD68 antibody (1:200 dilution, 28058–1-AP, Proteintech), anti-IBA1 antibody (1:100 dilution, CY7217, Abways), or anti-ST2 antibody (1:200 dilution, PRS3363, Sigma) at 4 °C overnight. Then, they were incubated with Cy3-labeled donkey anti-rabbit IgG (1:500 dilution, 111–165–003, Jackson) or Alexa Fluor 488-conjugated donkey anti-rabbit IgG(1:200 dilution, 111–165–003, Jackson) at RT for 1 h. The cell nuclei were stained with DAPI for 5 min. Immunoreactivity was observed using a fluorescence microscope. All images were analyzed with Image J software.

Statistical analysis

All statistical analyses were performed using SPSS 130.0 software. A Student's t-test was used to compare two groups for continuous variables with normal distributions. The differences in means among multiple groups were analyzed using a one-way analysis of variance (ANOVA). A probability (p) value of <0.05 was considered to indicate statistical significance.

Results

Protective effect of IL-33 on the NMOSD model

In the current study, purified human IgG from AQP4-IgG seropositive NMOSD patients were injected into the EAE mice to establish the NMOSD mice model (Saini et al., 2013). The timeline of model establishment is shown in Fig. 1**a**. HE staining showed prominent leukocyte infiltration around the lateral ventricle and in the subpial layer of the spinal cord of NMOSD mice. (Fig. 1**b**). The immunoreactivity of AQP4 was significantly decreased in the spinal cord of the NMOSD mice compared to those in the control and EAE mice (Fig. 1**c**). Co-staining with anti-AQP4 antibody revealed co-localization with anti-human antibody, especially around the blood vessels in the brain tissues of NMOSD mice (Supplementary figure 1).

To investigate the effect of IL-33 on NMOSD mice, we intraperitoneally injected IL-33 (50 ng) into NMOSD mice for consecutive 3 days before the start of model induction. During the establishment of the model, the body weight of animals in the control group steadily increased, while that in the NMOSD model decreased with time. IL-33 pretreatment gradually increased body weight in the NMOSD mice (Fig. 2**a**). After the model was established, the animal clinical score was studied. The NMOSD mice developed symptoms, such as tail or limb weakness, and the clinical score was significantly increased compared to that of the control mice (Fig. 2**b**). However, the IL-33 pretreatment decreased the clinical score in NMOSD mice. LFB staining showed notable demyelination in the brain of the NMOSD mice compared to that in the control mice (Fig. 2**c**). Immunofluorescence staining showed decreased NeuN expression in the EAE and NMOSD mice compared to that in the control mice. Pretreatment with IL-33 in the NMOSD mice significantly ameliorated brain NeuN loss and demyelination (Fig. 2**c and d**).

Next, transmission electron microscopy (TEM) was performed to check whether IL-33 pretreatment could protect against neuronal damage. Representative TEM images show that clear and dense myelin sheaths in the control group, while loose myelin sheaths with lamellar separation in the NMOSD mice (Fig. 3**a**). A significantly higher G-ratios were observed in NMOSD group, which could be ameliorated by pretreatment with IL-33 (Fig. 3**d**). In addition, astrocytes with dark nuclei and condensed chromatin were found in the NMOSD mice (Fig. 3**b**). IL-33-pretreated mice exhibited less axon damage and astrocyte disorder than the EAE and NMOSD mice (Fig. 3**a and b**). The control mice exhibited an intact mitochondrial structure with clear cristae ridges. Conversely, the NMOSD mice showed marked swelling mitochondrial structure, which could be ameliorated by IL-33 pretreatment (Fig. 3**c**).

Microglia pretreated with IL-33 alleviated the neuronal injury induced by NMOSD serum in vitro

To investigate whether IL-33 can alleviate the neuronal injury induced by NMOSD serum, BV2 cells, pretreated with IL-33 for 24 h, were treated with NMOSD serum and cocultured with rat primary cortical neurons. After 48 h of coculture, the supernatants were collected, and the concentrations of inflammatory cytokines were analyzed by ELISA. The results revealed that compared to the control and IL-33-treated groups, the levels of IL-1β, IL-6, and TNF-α were dramatically increased. That of IL-10 was dramatically decreased in the

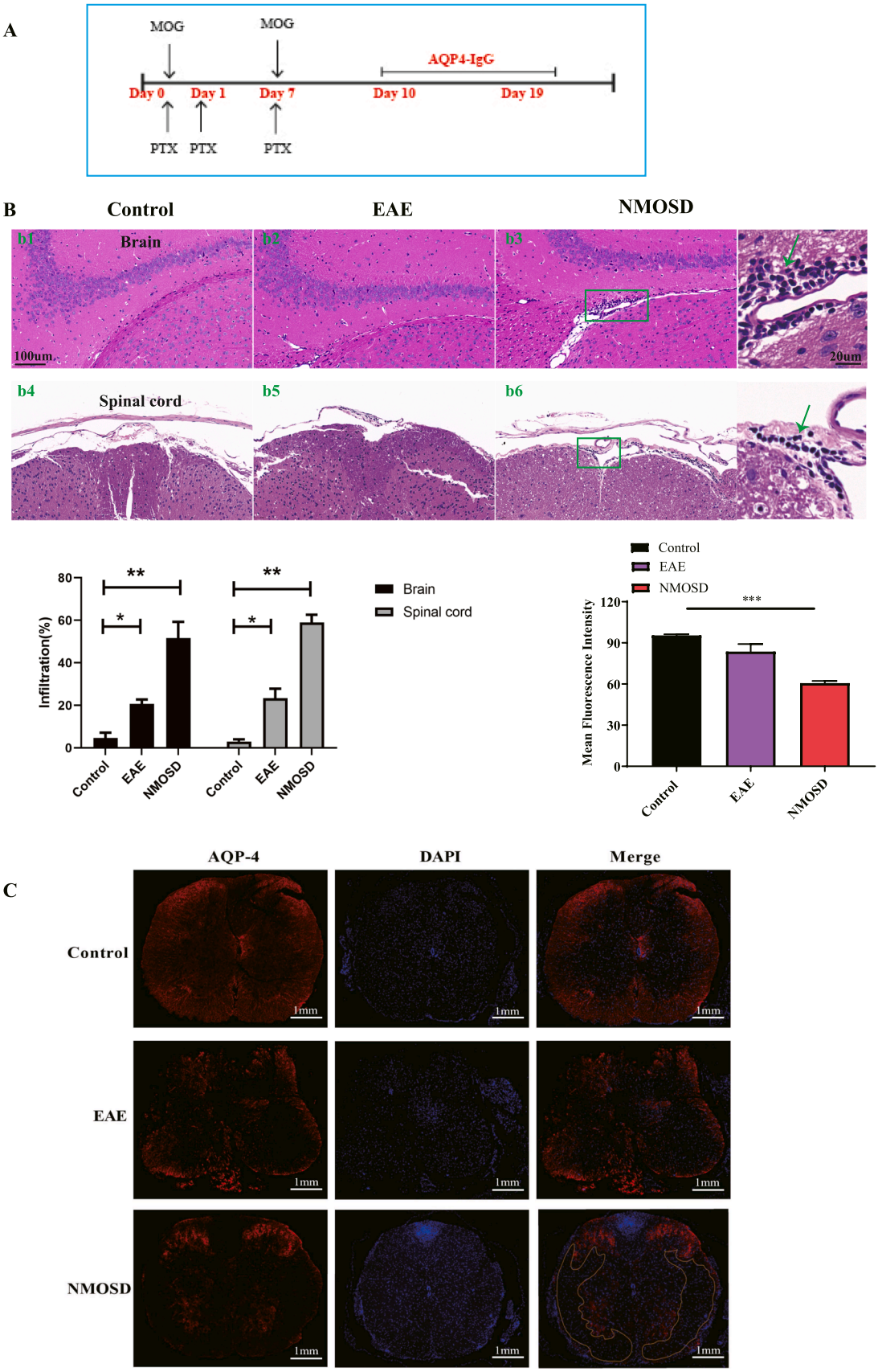

Fig. 1. Establishment of the NMOSD model. (**a**) Timeline of the establishment of the NMOSD model. PTX, Pertussis toxin. (**b**) HE staining and infiltration percentages of the brain and spinal cord in the control, EAE, and NMOSD mice. Scale bar = 100 μm. (**c**) AQP-4 expression was observed by immunostaining in the spinal cords of control, EAE, and NMOSD mice. Scale bar = 1 mm. One-way analysis of variance was used for statistical analyses. ***p<0.001.

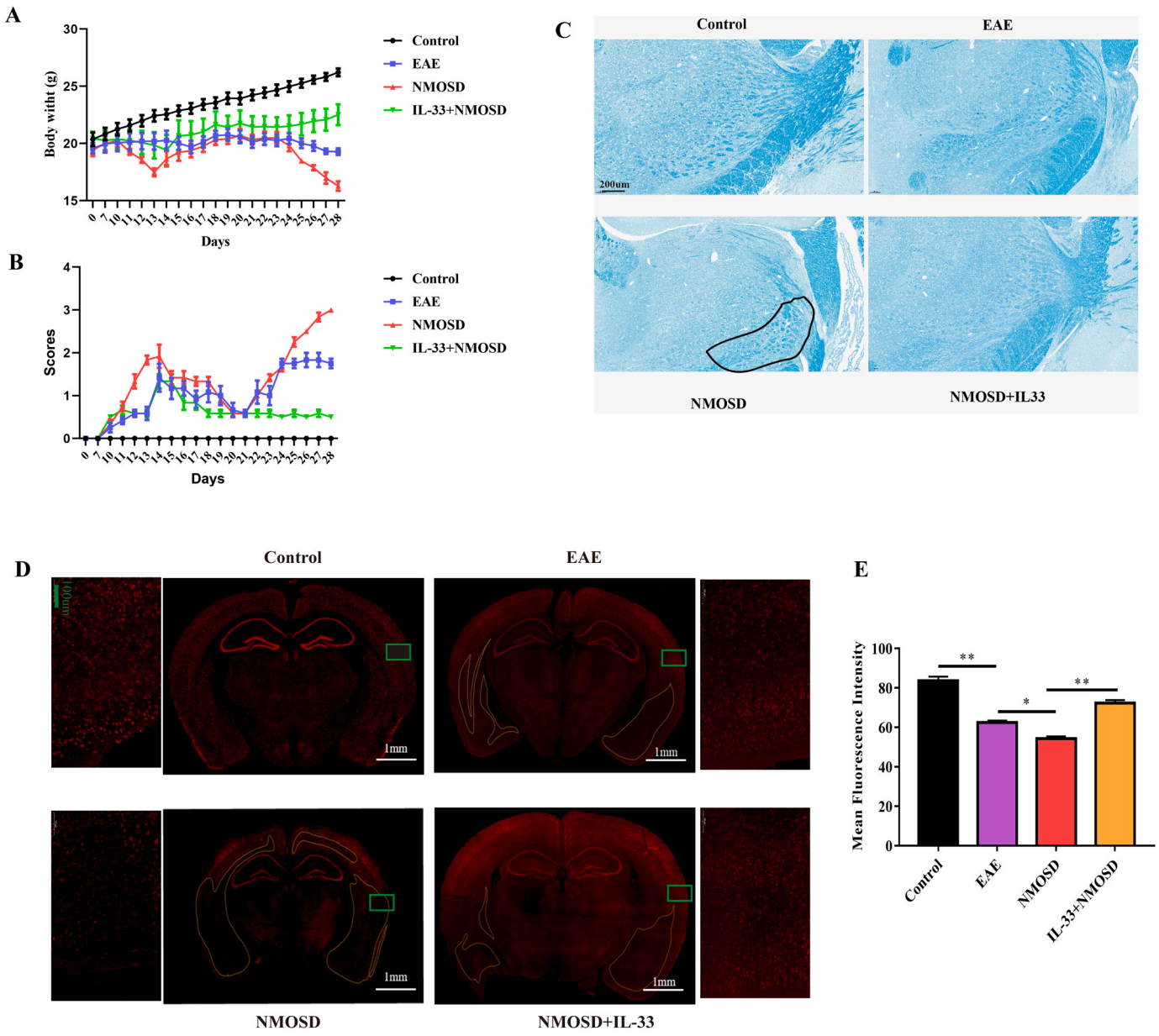

Fig. 2. Protective effect of IL-33 on NMOSD mice. (**a**) Body weight changes of the experimental animals. (b) Assessment of clinical scores for the experimental animals. (**c**) LFB staining of the brain. Scale bar = 200 μm. (**d**) Expression of NeuN was observed via immunofluorescence staining. Scale bar = 1 mm. One-way analysis of variance was used for statistical analyses. *p<0.05, **p<0.01.

NMOSD serum-treated group, which was reversed by pretreatment with IL-33 (Fig. 4**a**). In addition, immunofluorescence results suggested that the morphology of the neurons was damaged in the NMOSD serum group and recovered to normal after pretreatment with IL-33, as evidenced by PSD 95 protein expression levels (Fig. 4**b**). These results indicate that in the coculture system, pretreatment with IL-33 in microglia alleviated NMOSD serum-induced inflammation and damaged morphology in the cultured neurons.

Microglia were activated and transformed to the M2 phenotype after treatment with IL-33

To elucidate the effect of IL-33 on microglia, BV2 cells were treated with IL-33 or NMOSD serum separately. Western blotting results showed that compared with the control group and the NMOSD serum group, the IL-33 treatment significantly increased CD206 expression in M2 microglia. Compared to the control group, both the NMOSD serum and IL-33 treatments increased CD40 expression levels, but the levels were higher in the serum treatment group (Fig. 5**a**). Meanwhile, compared with the control group, both IL-33 and NMSOD serum treatments increased Iba-1 expression in the BV2 cells. Moreover, compared with the IL-33-treated group, several more M1 phenotypes were observed in the NMOSD serum-treated group, as suggested by the enlarged branching cell bodies (Fig. 5**b**). Immunofluorescence staining revealed that the NMOSD serum treatments significantly increased CD68 immunoreactivity compared to that in the control and IL-33 groups (Fig. 5**c**). This phenomenon revealed that both NMOSD serum and IL-33 treatments activated microglia; however, they led to different outcomes. IL-33 transformed microglia to the M2 phenotype, whereas the NMOSD serum promoted microglia to the M1 phenotype.

IL-33 treatment increased ST2 expression

To investigate the effects of IL-33 treatment on gene expression in

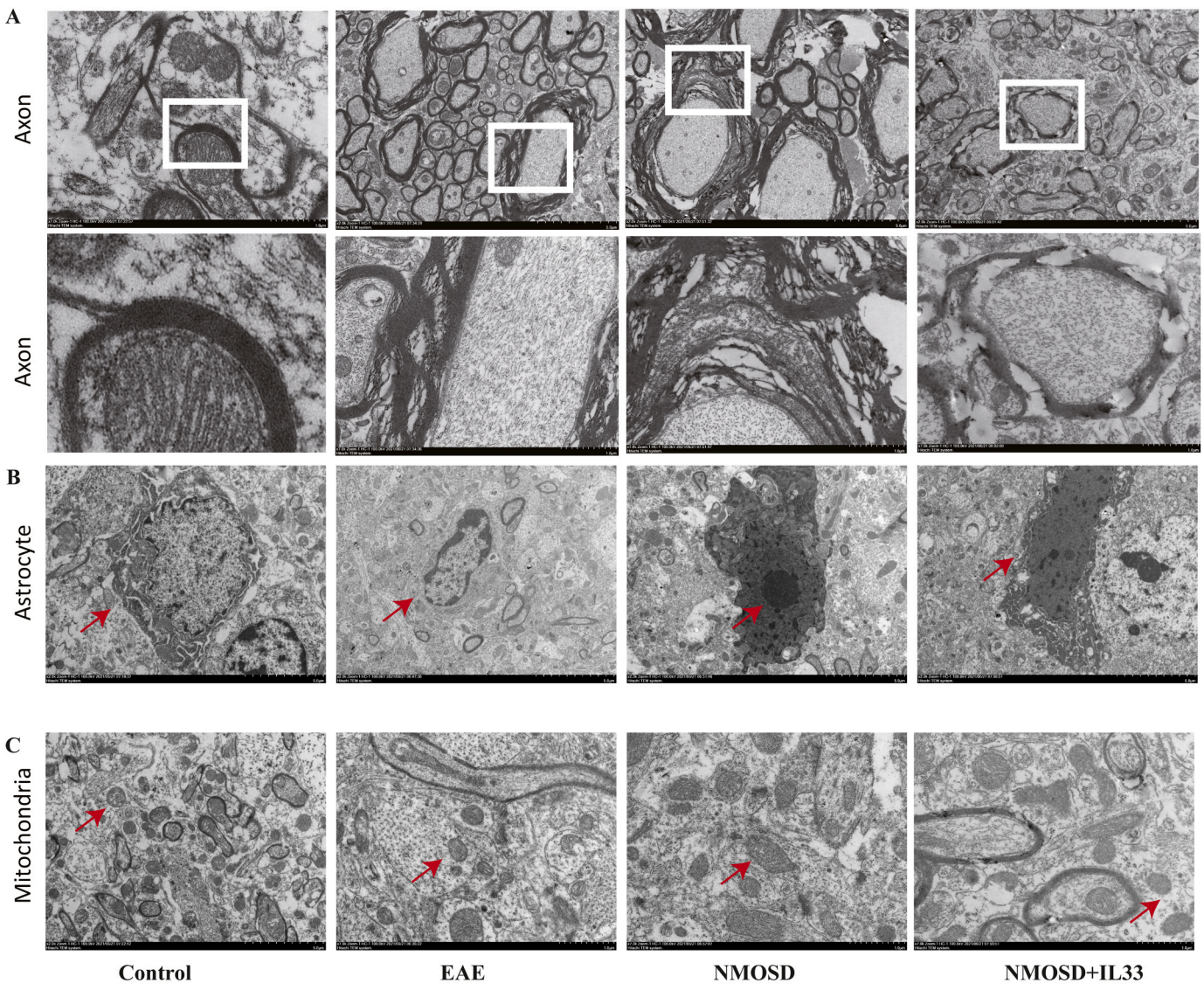

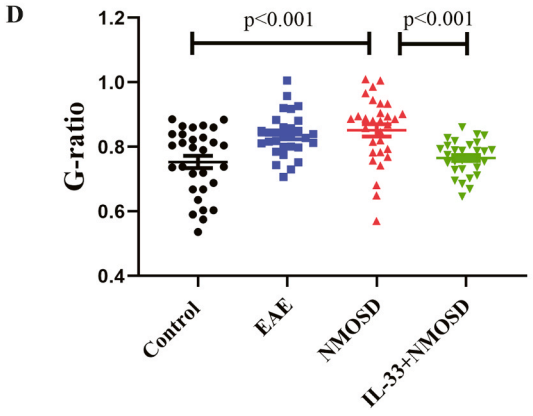

Fig. 3. IL-33 pretreatment ameliorated axon, astrocyte, and mitochondrial injury in NMOSD mice. **(A-C)** Structure of axon, astrocyte, and mitochondria were observed by TEM in the brains of the control, EAE, NMOSD, and NMOSD + IL-33 mice. (D) G-ratios of the control, EAE, NMOSD, and NMOSD + IL-33 mice.

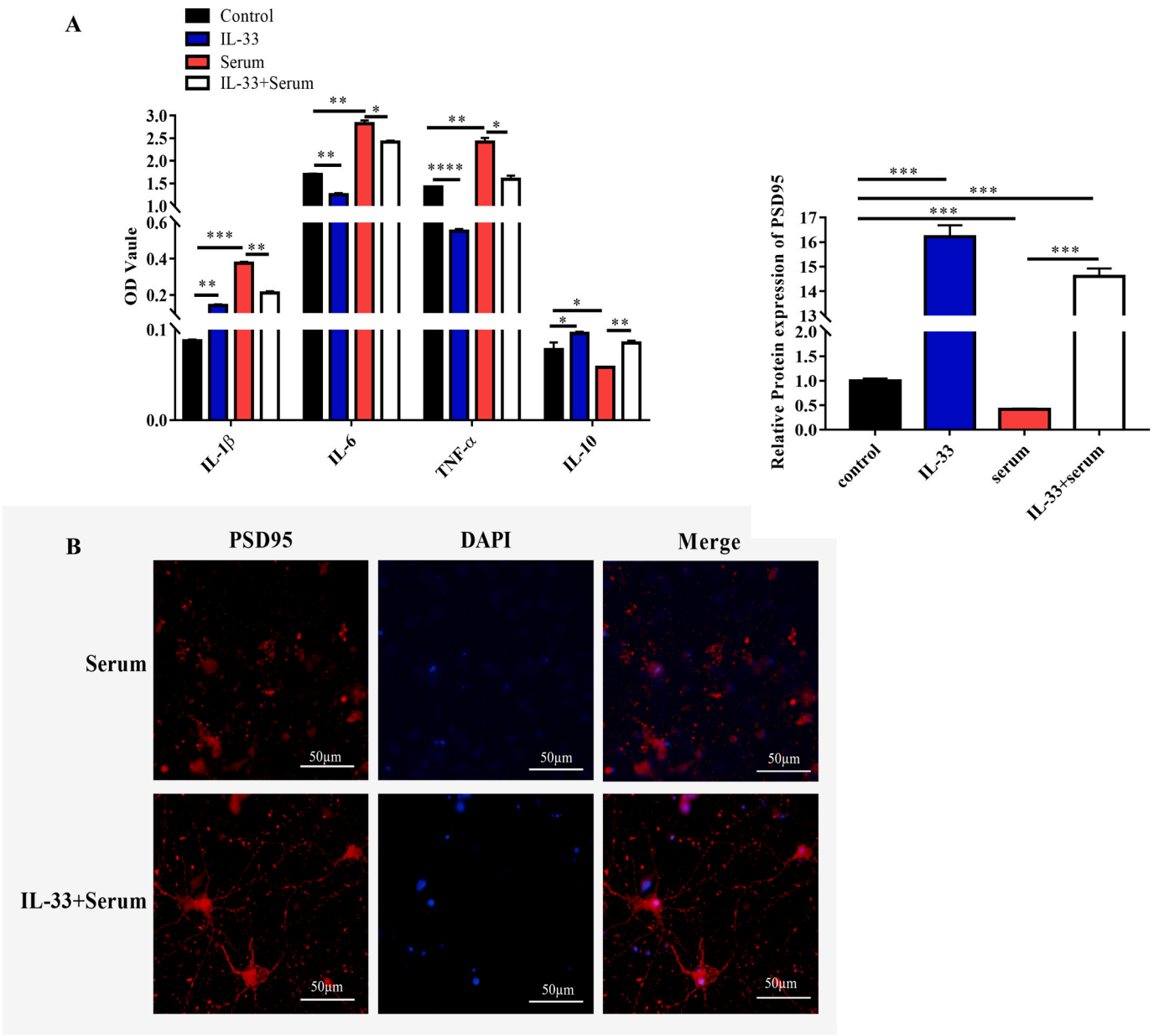

Fig. 4. IL-33 pretreatment protected against neuroinflammation and neuronal injury. (**a**) Levels of IL-1β, IL-6, TNF-α, and IL-10 were detected in cell cultures using ELISA kits and the control, IL-33, NMOSD serum, and NMOSD serum + IL-33 treatment groups. (**b**) PSD-95 expression levels in neuronal cells were studied by IFA after the cells were treated with IL-33 and serum. One-way analysis of variance was used for statistical analyses. *p<0.05, **p<0.01, ***p<0.001.

BV2 cells, we collected the cell supernatants and performed total mRNA sequencing analysis after 24 h of IL-33 treatment. The clustering heatmap and volcano images show that the expression of a series of genes was altered between the control and IL-33-treated groups (Fig. 6**a and b**). The most altered genes that are related to IL-33 are labeled in Fig. 6**b**. ST2, an IL-1 receptor family member, which is also known as Il1rl1, and its ligand IL-33 play important roles in immune regulation and inflammatory responses (Fairlie-Clarke et al., 2018). The mRNA level of ST2, was significantly upregulated in the IL-33 group compared to that in the control group (Fig. 6**c**). In addition, the protein levels of ST2 were significantly increased in the 50 and 100 ng/mL IL-33-treated groups compared to the control group and 200 ng/mL IL-33-treated group (Fig. 6**d**). The immunoreactivity of ST2 was significantly increased in the IL-33 group (100 ng/mL) compared to that of the control group (Fig. 6**e**). All these results indicate that IL-33 treatment increases the mRNA and protein levels of ST2 in BV2 cells.

IL-33 mediated microglial polarization via ST2

To investigate the mechanism of microglial polarity, a BV2 cell line with ST2 knockdown was used. A decrease in ST2 was demonstrated at both the mRNA and protein levels in the ST2-knockdown cells (Fig. 7**a and b**). Meanwhile, the decrease in ST2 led to a reduction in the Iba-1 protein (Fig. 7**b**). However, the synergistic effect of IL-33 on CD206 was significantly alleviated in the ST2-knockdown cells (Fig. 7**c**), which suggests that the M2 phenotype microglia were reduced after the knockdown of ST2. These results indicate that IL-33 affects microglial polarity via the ST2 pathway.

Discussion

IL-33 is an immunomodulatory cytokine that plays critical roles in tissue function and immune-mediated diseases (Cayrol and Girard, 2022). Previous clinical studies showed that the serum level of IL-33

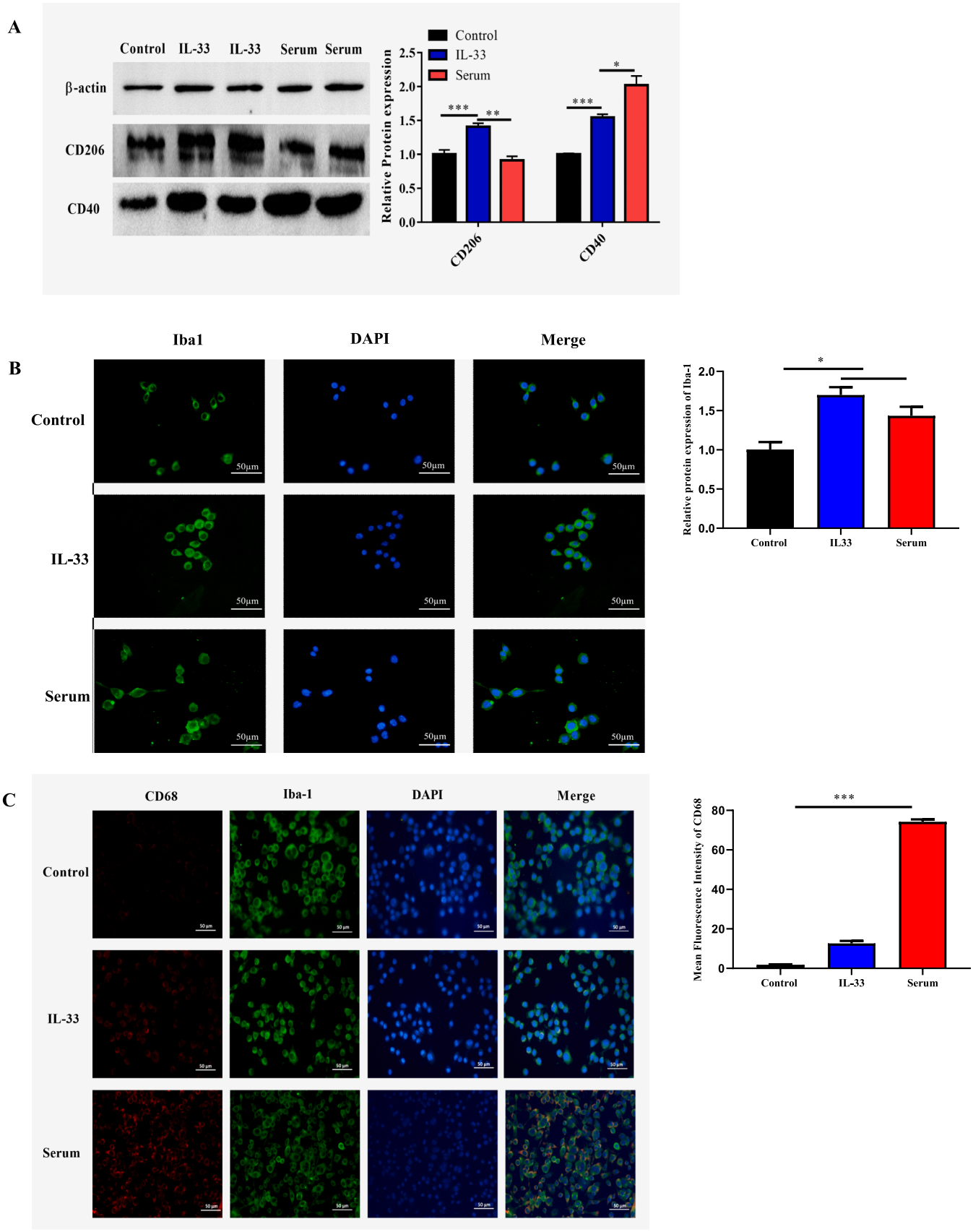

Fig. 5. Microglial cells were activated and transformed to the M2 phenotype after treatment with IL-33. **(a)** Western blot images and the quantification of CD206 and CD40 levels after treatment with IL-33 or NMOD serum. **(b)** BV2 cells were labeled with Iba-1 and CD68 for immunofluorescence. **(c)** Expression levels of PSD95 were observed by immunofluorescence after treatment with IL-33 or NMOSD serum. One-way analysis of variance was used for statistical analyses. *p<0.05, **p<0.01, ***p<0.001.

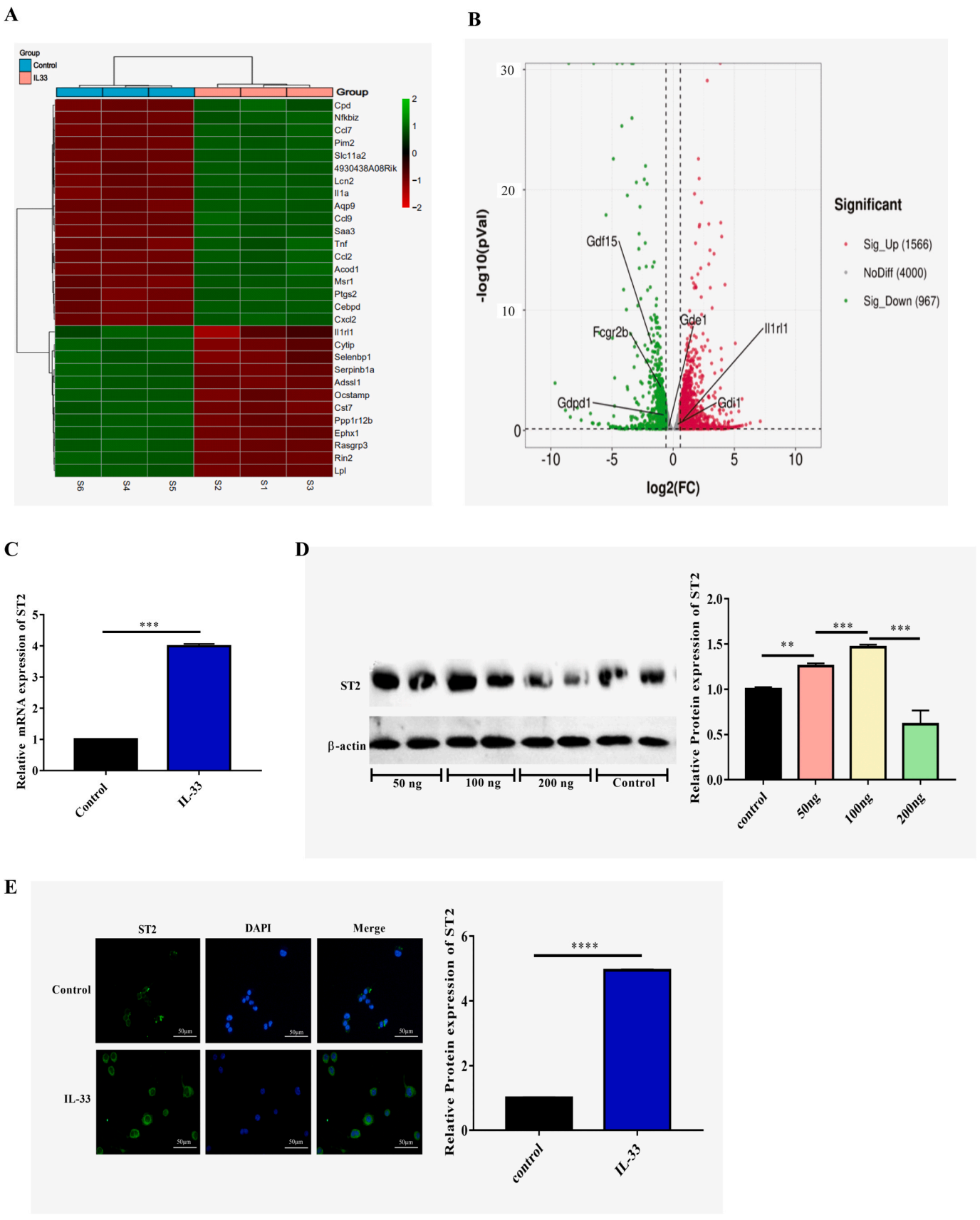

Fig. 6. Expression level changes of ST2 after treatment with IL-33. (**a**) Clustering heatmap showing the differentially expressed genes between the control and IL-33 treatment groups. (**b**) Volcano plot showing the differentially expressed genes between the control and IL-33 treatment groups. (**c**) mRNA levels of ST2 in the control and IL-33 treatment groups. (**d**) Western blot images and quantification of the ST2 levels after treatment with different concentrations of IL-33. (**e**) Immunofluorescence images showing the expression of ST2 after IL-33 treatment. A Student's t-test was used for statistical analyses. ***p<0.001.

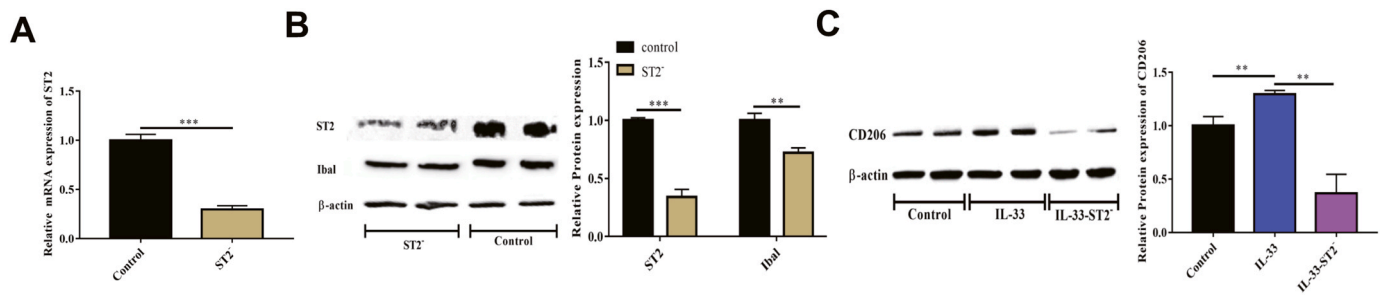

Fig. 7. IL-33 mediates microglial cell polarization by targeting ST2. **(a)** Silencing efficiency of ST2 at the mRNA level was analyzed by qPCR. **(b)** Protein expression levels of Iba-1 and ST2 were tested by immunoblotting after ST2 knockdown. **(c)** Expression of CD206 was investigated using western blotting following IL-33 treatment and IL-33 treatment + ST2 silencing. A Student's t-test or one-way analysis of variance was used for statistical analyses. **p<0.01, ***p<0.001.

during the acute phase was associated with more past attacks in patients with NMOSD (Zhang et al., 2018); however, the underlying mechanism has been inadequately investigated to date. Though the neuroprotective effect of IL-33 has been reported in animal models of spinal cord injury (Pomeshchik et al., 2015) and ischemic brain injury (Korhonen et al., 2015; Xie et al., 2022), little is known about its function in the NMOSD mice model. In the single existing study related to this, Kong et al. identified a significant reduction of group 2 innate lymphoid cells (ILC2) in the peripheral blood of NMOSD patients and the expansion of ILC2 by IL-33 treatment ameliorated the pathology of NMOSD mice (Kong et al., 2021). The current study provides the first evidence that IL-33 can protect against NMO pathology through the IL-33/ST2 pathway. Herein, we revealed that pretreatment with IL-33 protected against body weight and neuron loss, and alleviated clinical symptoms in NMOSD mice. Using TEM, we observed that the IL-33 pretreatment improved the structure of neurons, astrocytes, axons, and mitochondria in NMOSD mice. This study also suggested that pretreatment with IL-33 in microglia in the coculture system alleviated NMOSD serum-induced inflammation and damaged morphology in the cultured neurons.

Microglia play crucial roles in NMOSD (Chen et al., 2021). Microglia can be activated and polarized to the M1 phenotype by stimulating immunoglobulin or complement in the serum. After activation of the microglia from the resting state to the M1 phenotype, the branching cell body becomes larger and less swollen (Chu et al., 2018). M1 microglia are proinflammatory and release proinflammatory cytokines, such as IL-6, IL-1 beta, and TNF-alpha. By contrast, the M2 phenotype contributes to tissue repair and releases anti-inflammatory cytokines (Tian et al., 2022).

Several studies have reported the function of IL-33/ST2 signaling in microglial polarization in CNS diseases. Previous research found that IL-33 treatment reduced EAE myelitis by shifting the Th17/Th1 response to Th2 activity and polarizing anti-inflammatory M2 macrophages (Jiang et al., 2012). Fu et al. reported that IL-33 treatment modulated the innate immune response through polarizing microglia to an anti-inflammatory phenotype (M2) and reducing proinflammatory gene expression in APP/PS1 mice (Fu et al., 2016). Another study identified that the loss of ST2 enlarged brain lesion sizes in stroke models, and the activation of IL-33/ST2 signaling in the ischemic brain resulted in M2 microglial polarization, which in turn protected the ischemic neurons in an IL-10-dependent manner (Wang et al., 2017). These reports indicate the possibility that the neuroprotective function of IL-33 on NMOSD is correlated with microglial polarization. The results of the current study revealed that in cultured BV2 cells, both IL-33 and NMOSD serum activated the microglia individually. Meanwhile, IL-33 increased the levels of the M2 markers CD206 and IL-10, while NMOSD serum increased the levels of the M1 marker CD40 and other proinflammatory cytokines (such as IL-1 beta, IL-6, and TNF-alpha). Furthermore, using ST2 knockdown cell lines, we demonstrated that the role of IL-33 in promoting the polarization of microglia to the M2 phenotype was dependent on ST2.

There are a few limitations of our study. First, under high dose of IL-33 (200 ng/mL), the level of ST2 was significantly decreased compared to that under the low doses (50 and 100 ng/mL). Further study needs to explore the reason for this phenomenon. Second, additional behavioural tests, such as rotarod test and balance beam test, would help validate the protective effect on IL-33 on NMOSD mice. Third, the predominant type of lymphocytic cells ($CD4^+$or $CD8^+$ T lymphocytes) in the brain and spinal cord of NMOSD mice should be identified by immunostaining.

Ethics approval

This study was approved by the committees for ethical review of research involving human and animals subjects at the Second Affiliated Hospital of Guangzhou Medical University (Guangzhou, China). Written informed consent was obtained from all participants.

CRediT authorship contribution statement

Congcong Fu: Funding acquisition, Writing – original draft. **Sha Liao:** Methodology, Project administration. **Lu Huang:** Data curation, Conceptualization, Project administration. **Youming Long:** Conceptualization, Writing – review & editing.

Appendix A. Supporting information

Supplementary data associated with this article can be found in the online version at doi:10.1016/j.ibneur.2024.07.008.

References

Cayrol, C., Girard, J.P., 2022. Interleukin-33 (IL-33): a critical review of its biology and the mechanisms involved in its release as a potent extracellular cytokine. Cytokine 156, 155891.
Chen, T., Bosco, D.B., Ying, Y., Tian, D.S., Wu, L.J., 2021. The emerging role of microglia in neuromyelitis optica. Front. Immunol. 12, 616301.
Chen, T., Lennon, V.A., Liu, Y.U., Bosco, D.B., Li, Y., Yi, M.H., et al., 2020. Astrocyte-microglia interaction drives evolving neuromyelitis optica lesion. J. Clin. Investig. 130, 4025–4038.
Chu, F., Shi, M., Zheng, C., Shen, D., Zhu, J., Zheng, X., et al., 2018. The roles of macrophages and microglia in multiple sclerosis and experimental autoimmune encephalomyelitis. J. Neuroimmunol. 318, 1–7.
Fairlie-Clarke, K., Barbour, M., Wilson, C., Hridi, S.U., Allan, D., Jiang, H.R., 2018. Expression and function of IL-33/ST2 axis in the central nervous system under normal and diseased conditions. Front. Immunol. 9, 2596.
Fu, C.C., Gao, C., Zhang, H.H., Mao, Y.Q., Lu, J.Q., Petritis, B., et al., 2022. Serum molecular biomarkers in neuromyelitis optica and multiple sclerosis. Mult. Scler. Relat. Disord. 59, 103527.
Fu, A.K., Hung, K.W., Yuen, M.Y., Zhou, X., Mak, D.S., Chan, I.C., et al., 2016. IL-33 ameliorates Alzheimer's disease-like pathology and cognitive decline. Proc. Natl. Acad. Sci. USA 113, E2705–2713.
Guo, Y., Weigand, S.D., Popescu, B.F., Lennon, V.A., Parisi, J.E., Pittock, S.J., et al., 2017. Pathogenic implications of cerebrospinal fluid barrier pathology in neuromyelitis optica. Acta Neuropathol. 133, 597–612.
Hasselmann, J.P.C., Karim, H., Khalaj, A.J., Ghosh, S., Tiwari-Woodruff, S.K., 2017. Consistent induction of chronic experimental autoimmune encephalomyelitis in C57BL/6 mice for the longitudinal study of pathology and repair. J. Neurosci. Methods 284, 71–84.

Jiang, H.R., Milovanovic, M., Allan, D., Niedbala, W., Besnard, A.G., Fukada, S.Y., et al., 2012. IL-33 attenuates EAE by suppressing IL-17 and IFN-gamma production and inducing alternatively activated macrophages. Eur. J. Immunol. 42, 1804–1814.
Kong, Y., Li, H.D., Wang, D., Gao, X., Yang, C., Li, M., et al., 2021. Group 2 innate lymphoid cells suppress the pathology of neuromyelitis optica spectrum disorder. FASEB J.: Off. Publ. Fed. Am. Soc. Exp. Biol. 35, e21856.
Korhonen, P., Kanninen, K.M., Lehtonen, S., Lemarchant, S., Puttonen, K.A., Oksanen, M., et al., 2015. Immunomodulation by interleukin-33 is protective in stroke through modulation of inflammation. Brain Behav. Immun. 49, 322–336.
Long, Y., Liang, J., Zhong, R., Wu, L., Qiu, W., Lin, S., et al., 2017. Aquaporin-4 antibody in neuromyelitis optica: re-testing study in a large population from China. Int. J. Neurosci. 127, 790–799.
Lucchinetti, C.F., Guo, Y., Popescu, B.F., Fujihara, K., Itoyama, Y., Misu, T., 2014. The pathology of an autoimmune astrocytopathy: lessons learned from neuromyelitis optica. Brain Pathol. 24, 83–97.
Misu, T., Fujihara, K., Kakita, A., Konno, H., Nakamura, M., Watanabe, S., et al., 2007. Loss of aquaporin 4 in lesions of neuromyelitis optica: distinction from multiple sclerosis. Brain: A J. Neurol. 130, 1224–1234.
Pacifici, M., Peruzzi, F., 2012. Isolation and culture of rat embryonic neural cells: a quick protocol. Jove-J. Vis. Exp., e3965
Pomeshchik, Y., Kidin, I., Korhonen, P., Savchenko, E., Jaronen, M., Lehtonen, S., et al., 2015. Interleukin-33 treatment reduces secondary injury and improves functional recovery after contusion spinal cord injury. Brain Behav. Immun. 44, 68–81.
Saini, H., Rifkin, R., Gorelik, M., Huang, H., Ferguson, Z., Jones, M.V., et al., 2013. Passively transferred human NMO-IgG exacerbates demyelination in mouse experimental autoimmune encephalomyelitis. BMC Neurol. 13, 104.
Sun, Y., Ji, J., Zha, Z., Zhao, H., Xue, B., Jin, L., et al., 2021. Effect and mechanism of catalpol on remyelination via regulation of the NOTCH1 signaling pathway. Front. Pharmacol. 12, 628209.
Tian, Y., Liu, B., Li, Y., Zhang, Y., Shao, J., Wu, P., et al., 2022. viaActivation of RARα receptor attenuates neuroinflammation after SAH promoting M1-to-M2 PHenotypic Polarization of Microglia and Regulating Mafb/Msr1/PI3K-Akt/NF-κB pathway. Front. Immunol. 13, 839796.
Vainchtein, I.D., Chin, G., Cho, F.S., Kelley, K.W., Miller, J.G., Chien, E.C., et al., 2018. Astrocyte-derived interleukin-33 promotes microglial synapse engulfment and neural circuit development. Science 359, 1269–1273.
Wang M., Xia D., Sun L., Bi J., Xie K., Wang P. Interleukin-33 as a biomarker affected intrathecal synthesis of immunoglobulin in NMOSD and MOGAD. European neurology 2023.
Wang, S., Yang, T., Wan, J., Zhang, Y., Fan, Y., 2017. Elevated C-X-C motif ligand 13 and B-cell-activating factor levels in neuromyelitis optica during remission. Brain Behav. 7, e00648.
Wlodarczyk, A., Khorooshi, R., Marczynska, J., Holtman, I.R., Burton, M., Jensen, K.N., et al., 2021. Type I interferon-activated microglia are critical for neuromyelitis optica pathology. Glia 69, 943–953.
Xie, D., Miao, W., Xu, F., Yuan, C., Li, S., Wang, C., et al., 2022. IL-33/ST2 axis protects against traumatic brain injury through enhancing the function of regulatory T cells. Front. Immunol. 13, 860772.
Yao, X.Y., Wu, Y.F., Gao, M.C., Hong, R.H., Ding, J., Hao, Y., et al., 2020. Serum albumin level is associated with the severity of neurological dysfunction of NMOSD patients. Mult. Scler. Relat. Disord. 43, 102130.
Zhang, Y., Yao, X.Y., Gao, M.C., Ding, J., Hong, R.H., Huang, H., et al., 2018. Th2 axis-related cytokines in patients with neuromyelitis optica spectrum disorders. CNS Neurosci. Ther. 24, 64–69.